# A quality assurance program for an amorphous silicon electronic portal imaging device using in-house developed phantoms: a method development for dosimetry purposes

**A. Jomehzadeh[1,2*], P. Shokrani[1], M. Mohammadi[3,4], A. Amouheidari[5]**

*[1] Medical Physics Department, Isfahan University of Medical Sciences, Isfahan, Iran*
*[2] Medical Physics Department, Rafsanjan University of Medical Sciences, Rafsanjan, Iran*
*[3]Medical Physics Department, Hamadan University of Medical Sciences, Hamadan, Iran*
*[4] Medical Physics Department, Royal Adelaide Hospital. Adelaide, SA 5000, Australia*
*[5]Radiation Oncology Department, Isfahan Milad Hospital, Isfahan, Iran*

► ***Original article***

**** Corresponding author:***
*Dr. Ali Jomehzadeh,*
***Fax:*** *+98 391 5225209*
***E-mail****: jomehzadeh@rums.ac.ir*

**Received:** March 2013
**Accepted:** June 2013

***Int. J. Radiat. Res., July 2014; 12(3): 257-264***

## ABSTRACT

***Background***: Electronic portal imaging devices (EPIDs) play an important role in radiation therapy portal imaging, geometric and dosimetric verifications. A successful utilization of EPIDs for imaging and dosimetric purposes requires a reliable quality control process routine to be carried out regularly. In this study, two in-house phantoms were developed and analyzed for implementation in a quality assurance program for dosimetry purposes. ***Materials and Methods***: An amorphous silicon (a-Si) imager (OptiVue500) was used. A low contrast resolution phantom and an image quality phantom were constructed and implemented. Low contrast resolution of the EPID was evaluated by counting the number of holes detectable in the image of phantom using human observers and a software. The image quality phantom was used for modulation transfer function, contrast to noise ratio and noise level evaluations. This phantom contains five sets of high-contrast rectangular bar patterns of variable spatial frequencies and six uniform regions. ***Results***: Although the manual low contrast resolution method was observer-dependent and insensitive to artifacts, the automatic method was robust and fully objective but sensitive to artifacts. The critical frequency values for 6 and 18 MV were 0.3558±0.006 *lp/mm* and 0.2707±0.006 *lp/mm* respectively. The contrast-to-noise ratio was found to be ~ 240% higher for 6 MV compared to 18 MV. ***Conclusion***: The developed phantoms provide a convenient process for periodic performance of an EPID. These phantoms are independent of the EPID system and provide robust tools for continuous monitoring of image quality parameters as well as dosimetric parameters.

***Keywords:*** *Electronic portal imaging device, quality assurance, phantom.*

## INTRODUCTION

The goal in radiotherapy is to achieve the highest degree of conformity in delivering the dose to the target and minimum dose to the organs at risk. To achieve this goal, advanced radiation treatment techniques, such as Intensity Modulated Radiation Therapy (IMRT) [1, 2], Volumetric Modulated Arc Therapy (VMAT) [3, 4] and Image Guide Radiation Therapy [5], have been implemented. An accurate treatment delivery using these techniques is not possible without accurate patient positioning and dose delivery verifications [2-6]. Portal imaging, using electronic portal imaging devises (EPIDs), has been addressed as a key element for the above

mentioned verifications [6-8]. Modern linear accelerators (linacs) are equipped with advanced EPIDs which utilize amorphous silicon (a-Si) detection technology. A-Si EPIDs provide a superior image quality compared to the other types of EPIDs [9].

Although, EPIDs were initially introduced for verification of patient positioning in radiation therapy [10-21], they have recently been used for dosimetric purposes [11-16, 21-26], quality control (QC) of multi leaf collimator (MLC) or verification of gantry angle for IMRT and VMAT quality assurance (QA) [27, 28]. A successful utilization of EPIDs for imaging and dosimetric purposes requires a reliable quality control process to be carried out regularly [29-33].

The American Association of Physicist in Medicine (AAPM) Task Group-58 (TG-58) has recommended a daily check of imaging functionality and a monthly check of image quality for EPIDs[29]. It also highlights the importance of assessing clinical image quality by measuring the spatial resolution and contrast of the EPID.

The accuracy required for dosimetry purposes in modern radiation therapy demands consistent image quality and quantitative tests that are robust, precise, accurate and automatic. For example the minimum baseline of critical frequency ($f_{50}$) required for dosimetry purposes for low energy and high dose rate is 0.33 *lp/mm* [34]. Since the accuracy criteria for an EPID-based dosimetry protocol is more stringent than a positioning verification protocol, it is important to establish a QA protocol for dosimetry applications to monitor EPID performance as a regular, defined frequency [29].

The main three phantoms originally used in the assessment of EPID image quality are, Las Vegas phantom [31], PIPSPro QC-3V phantom[32] and PTW EPID QC phantom[9].

The main limitation associated with using the Las Vegas phantom include subjective process of image visualization, i.e., dependency of the process to viewing conditions, monitor performance and observer training [35]. On the contrary, PIPSPro QC-3V phantom provides quantitative analysis of image contrast, noise and spatial resolution using the epidSoft software analysis [9, 34] . The main drawback of PTW EPID QC phantom include the phantom size which is too large for the Varian image detector [9].

The primary aim of this work was to develop in-house phantoms with superior qualifications compared to existing phantoms and to develop a quality assurance program for an amorphous silicon electronic portal imaging devices (EPIDs) for dosimetry purposes.

## MATERIALS AND METHODS

### *The a-Si based EPID*

The EPID used in this work was an amorphous silicon (a-Si) flat panel imager (OptiVue500, Siemens Medical Solutions, Concord, USA) which is attached to a Siemens Oncor Impression medical linac. The imager has an active area of 41×41 $cm^2$ consisting of 512×512 pixels with a pixel size of 0.8 $mm^3$ [36].

### *Phantom1*

The Milad1 EPID prototype phantom (figure 1) was designed to follow customer acceptance procedure and consequently quality assurance checks. It is a 14×14×2.18 $cm^3$ block of aluminum which weights 1.2 Kg. A sequence of holes of varying diameters and depths were machined in the block. The holes in each row are located at the same depth, while holes in each column have the same diameters.

### *Phantom 2*

The Milad2 EPID phantom, which is shown in figure 2, was designed for quantitative analysis of image contrast (contrast-to-noise ratio), noise and spatial resolution of EPIDs. This phantom has dimensions of 13.5×11.3×3.6 $cm^3$ and incorporates two aluminum and acrylic slabs, each 1.5 cm thick, bonded together. The aluminum slab contains five sets of high-contrast rectangular bars, made of lead and paraffin, and has spatial frequencies of 0.1, 0.2, 0.25, 0.4 and 0.75 *lp/mm*. The central three bar patterns are surrounded by six uniform regions of lead, aluminum and paraffin of different thicknesses.

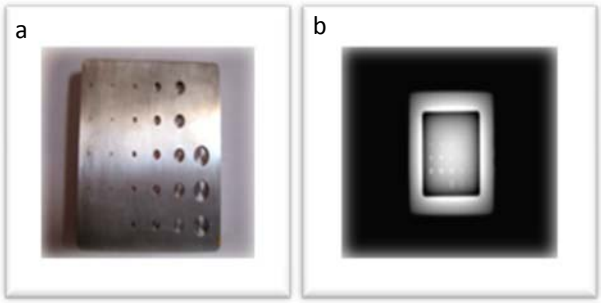


**Figure 1. a** The Milad1 EPID phantom, b. a portal image of the phantom.

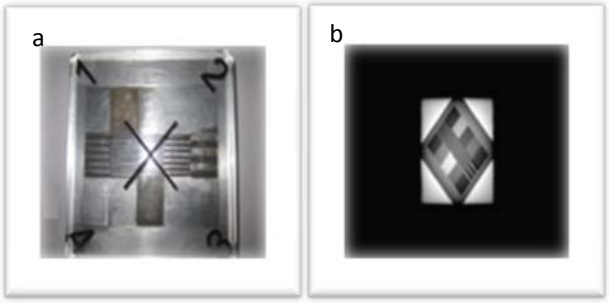


**Figure 2.** a. The Milad2 EPID Phantom, b. a portal image of the phantom.

### *Description of QA tests*

The QA program consisted of the following tests: evaluation of low contrast resolution and measurement of modulation transfer, contrast-to-noise ratio (CNR) and noise level for image quality assessments. The low contrast resolution was evaluated using Milad1 EPID phantom. The phantom was positioned on the surface of the EPID at source to imager distance (SID) of 130 cm with the holes facing the EPID, at gantry angle of 0°. For each acquisition mode two images were acquired and analyzed using two different methods of counting the holes: the visualization method and the automatic method. The visualization method is to count the number of holes visually by two trained observers. The window and level on the image display were adjusted to view the maximum number of holes for each acquisition mode [33]. The automatic method involved detecting different holes in an image using software. The software utilizes the programming language MATLAB 7.1 (The Mathworks Inc., Natick, MA) to detect the holes based on the difference between mean gray scale of each hole with its background.

### *Image quality*

Image quality parameters were measured quantitatively using Milad2 EPID phantom. The phantom was positioned on the surface of the EPID, at gantry angle of zero, SID=130 cm and at an angle of 45° with respect to the long axis of the treatment couch to prevent the spatial aliasing [33]. For each acquisition mode two images were acquired and analyzed to determine the relative modulation transfer function (RMTF), contract to noise ratio (CNR) and noise level.

Typically, the modulation transfer function (MTF) of an imaging system is taken to be the ratio of output to input modulation at varying spatial frequencies. RMTF is a similar measure, but renormalized by the MTF of the lowest frequency using the following equation:

$$RMTF(f) = \frac{MTF(f)}{MTF\left(0.1\frac{lp}{mm}\right)} \qquad (1)$$

Critical frequency ($f_{50}$) is defined as the spatial resolution corresponding to 50% RMTF [32].

A high quality image typically has a large CNR. This can be manipulated by increasing the contrast, decreasing the noise, or a combination of both. CNR is defined by the following equation:

$$CNR = \frac{I_b - I_a}{Noise} \qquad (2)$$

Where $I_b$ is the average pixel value in the areas receiving the least radiation, $I_a$ is the average pixel value in the areas receiving the most radiation dose, and *noise* represents the average of noise values calculated in the six uniformly irradiated regions of the phantom [30].

The images were analyzed objectively for spatial resolution, CNR and noise level using the PIPSpro software Version 4.4 (Standard Imaging Inc, USA). The PIPSpro software is included in the service software of the Siemens Coherence Therapist Workspace, the so called AQUA software.

## RESULTS

A total number of 144 images were acquired

and analyzed using the developed phantoms for 6 and 18 MV beams at different dose rate and 1, 2, 4, 6, 8, 10, 20, 30, 50 and 100 MUs. Due to a technical problem the images for 18 MV at dose rate of 50 *MU/min* were acquired for up to 30 MUs.

### *Low contrast resolution*

Figure 3 presents a comparison of the results obtained using the visualization and automatic methods of counting holes. The ranges of the obtained results using the first method versus the second method were as follows respectively:

For 6 MV at 50 *MU/min* 13.5-23 versus 4- 12, at 300 *MU/min* 14.5-23 versus 4-13, for 18 MV at 50 *MU/min* 10.5 - 16.5 versus 1-5 and at 500 MU 11-19.5 versus 2-11.

Also figure 3 shows that the average number of circles observed using the Milad1 EPID phantom was greater than the recommended tolerance of 17 [29], for all acquisition modes except for the following MU values: less than 4 for 6 MV at 300 *MU/min*, less than 20 for 18 MV at 500 *MU/min* and less than 6 and 10 for 6 and 18 MV at 50 *MU/min* respectively. Also the OptiVue 500 EPID provides superior low contrast resolution as recommended by AAPM TG-58 [29].

The average number of holes observed during the course of the study for the four acquisition modes is shown in table 1. The average number of holes observed is seen to increase at dose rates of 50, 300 *MU/min* for 6MV and at 50, 500 *MU/min* for $5^2$ MV. Also, it can be found that the mean number of holes decreases by increasing the beam energy for the same dose rate.

**Table 1.** Average number of holes observed (±1SD) for 6 and 18 MV at 50, 300 and 500 *MU/min*.

| Dose Rate [MU/min] | | | Energy [MV] |
|---|---|---|---|
| 500 | 300 | 50 | |
| ------ | 20.00±2.9 | 19.25±2.8 | 6 |
| 16.13±2.7 | ------ | 13.91±2.8 | 18 |

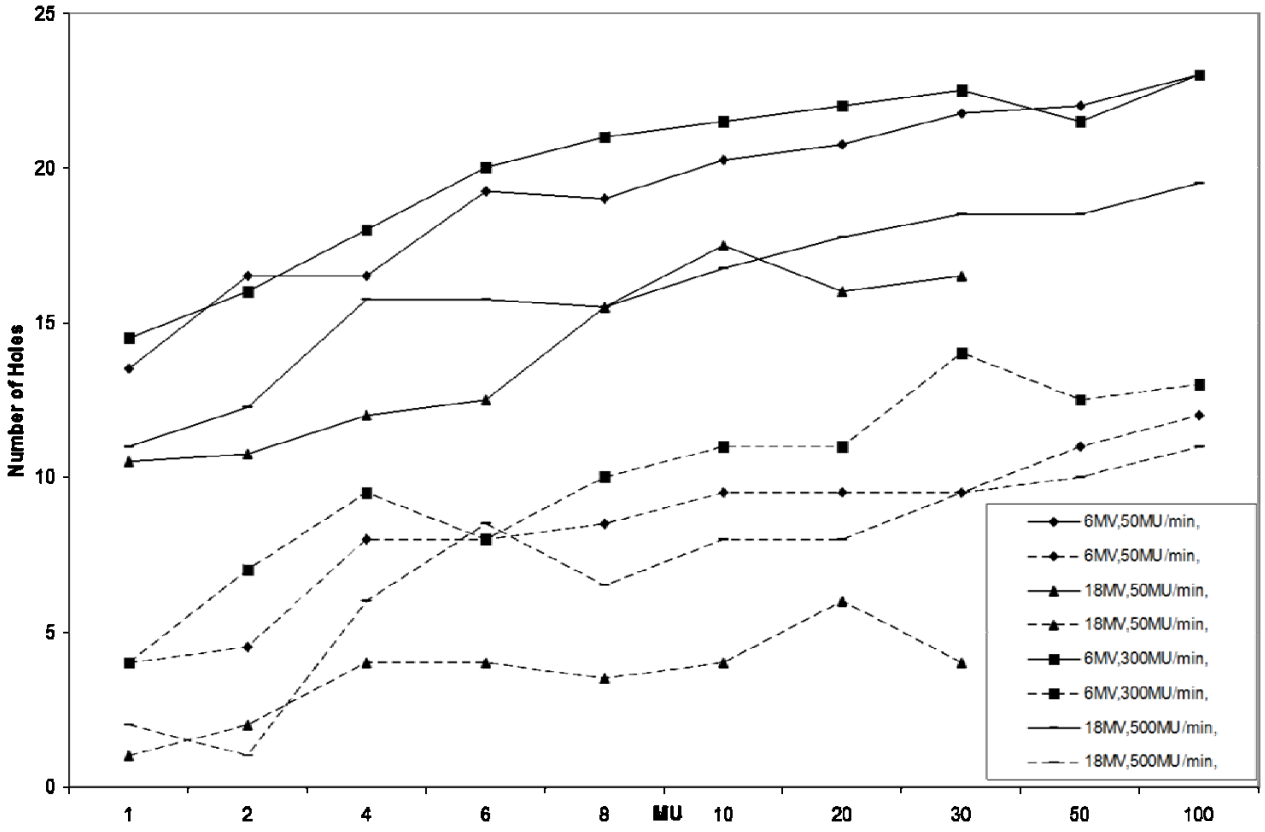


**Figure 3.** Milad1 EPID phantom test results: Number of holes detected using human observation (—) and software detection (---) for 6 and 18 MV at 50, 300 and 500 MU/min.

***Image quality***

The Milad2 EPID phantom was used to determine the critical frequency, contrast-to-noise ratio (CNR) and noise level for four different image acquisition modes. Figure 4 shows the values of $f_{50}$ as a function of MU obtained for 6 and 18 MV at three dose rates.

The Average values of $f_{50}$ were 0.3558±0.006 lp/mm and 0.2692±0.007 *lp/mm* for 6 and 18 MV, respectively. Also according to figure 4, the critical frequencies are independent of dose rate and number of MUs.

Figure 5 shows the variation of CNR with number of MUs for 6 and 18 MV at 50, 300 and 500 *MU/min*. The CNR value increases with dose rate and decreases with beam energy.

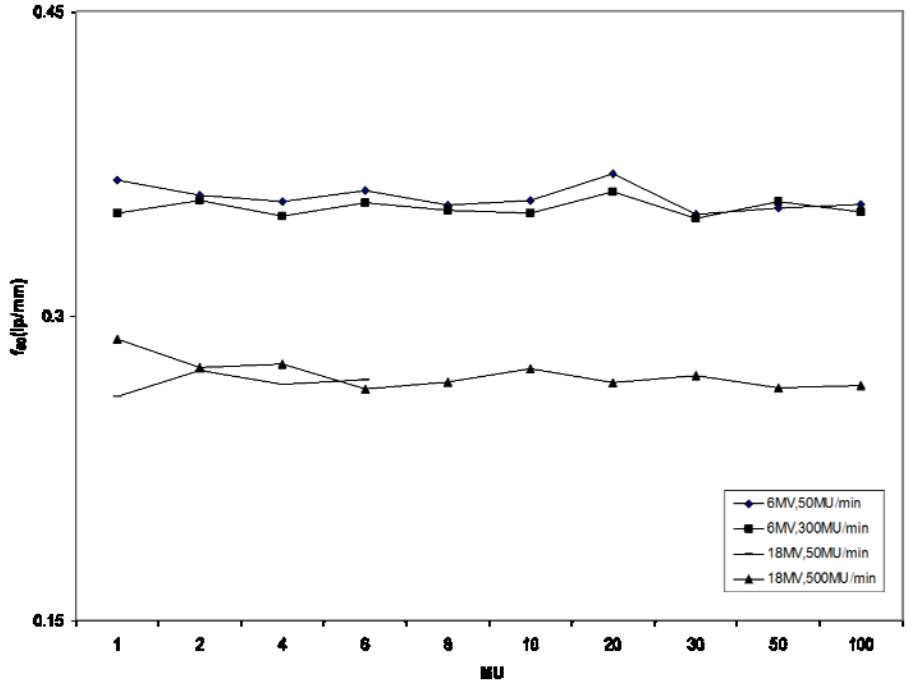


**Figure 4.** Variation of $f_{50}$ (lp/mm) as a function of MU for 6 and 18 MV at 50, 300 and 500 *MU/min*.

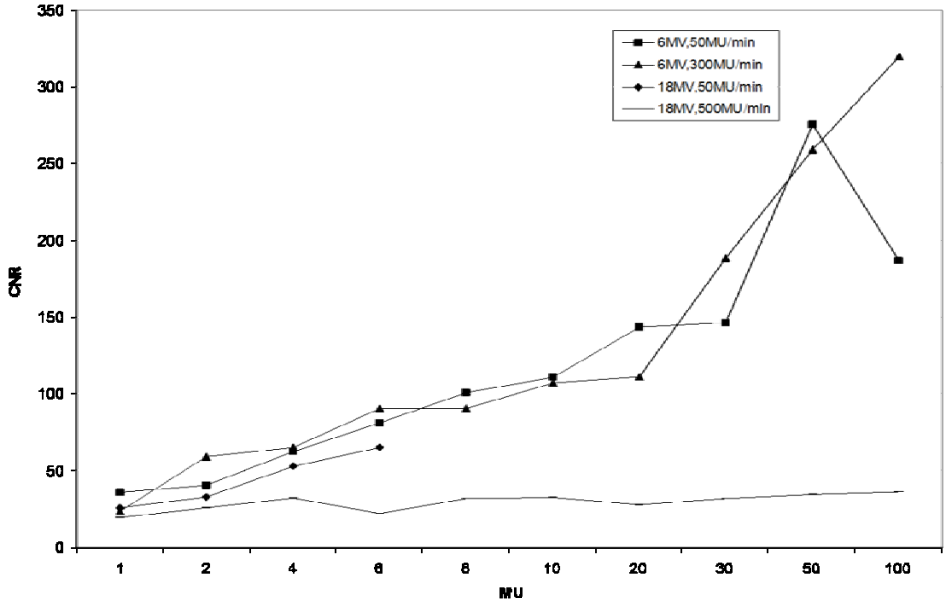


**Figure 5.** Variation of CNR versus number of MUs using Milad2 EPID phantom 6 and 18 MV at 50, 300 and 500 MU/min.

Figure 6 shows variation of CNR as a function of MUs obtained for 6 and 18 MV at three dose rates. It demonstrates a similar trend for CNR. Therefore CNR value correlates with the average number of holes visualized. The number of holes observed and CNR are seen to increase with MUs delivered.

Table 2 shows the mean of CNR and $f_{50}$ values obtained for 6 and 18 MV and different acquisition modes. An increase in CNR mean values was observed for dose rates of 50, 300 MU/min and 6 MV. Also the mean value of CNR and $f_{50}$ decreased with increase in beam energy. The average value of $f_{50}$ remained constant as a function of dose rate for both photon beam energy. It is also shown that CNR decreases with increase in beam energy.

**Table 2.** Average value of CNR and $f_{50}$ (±1SD) for 6 and 18 MV at 50, 300 and 500 *MU/min*.

| Energy [MV] | | Dose Rate [MU/min] | |
|---|---|---|---|
| 18 | 6 | | |
| 44.0±16.7 | 118.2±71.4 | 50 | CNR |
| ———— | 131.4±91.2 | 300 | |
| 29±24.1 | ———— | 500 | |
| 0.267±0.007 | 0.358±0.007 | 50 | $f_{50}$(lp/mm) |
| ———— | 0.353±0.005 | 300 | |
| 0.271±0.008 | ———— | 500 | |

The average and standard deviation of noise values for different MUs were 10.6±6.0 and 16.2±5.3 at dose rate of 50 *MU/min* for 6 and 18 MV respectively (table 3). Also the mean noise values were 43.3±17.3 and 103.7±25.2 for 6 MV at 300 *MU/min* and 18 MV at 500 *MU/min*. It is clear that by increasing dose rate and beam energy, noise in the image increases.

**Table 3.** Average of noise level (±1SD) for 6 and 18 MV at 50, 300 and 500 MU/min.

| Dose Rate [MU/min] | | | Energy [MV] |
|---|---|---|---|
| 500 | 300 | 50 | |
| _____ | 43.3±17.3 | 10.6±6.0 | 6 |
| 103.7±25.2 | _____ | 16.2±5.3 | 18 |

## DISCUSSION

In this study a QA program was development for an OptiVue500 EPID using two in-house developed phantoms. Low contrast resolution and image quality were determined. According to the data set achieved in the current study, the low contrast resolution does not show any dramatic change with machine parameters (see figure 3). The contrast resolution depends on the number of MUs delivered. Therefore,

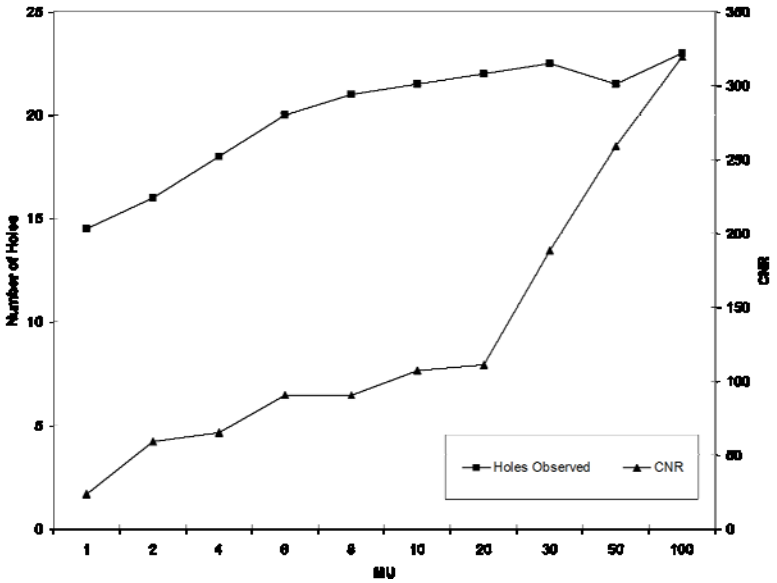


**Figure 6.** The number of holes observed and CNR as a function of MUs for 6 MV at 300 *MU/min*.

during routine EPID QA it is important to consider the minimum number of MUs required for acceptable low contrast resolution. The number of holes detected in the images exposed under similar conditions depends on the detection method. While the software method of counting holes is noise dependent, the standard method is observer dependent and independent of noise. Our results for contrast resolution are superior to those reported by Menon *et al.* for an a-Si EPID, where the number of holes detected at a dose rate of 300 MU/min were 16.9±1.2 for 6 MV[31]. The average values of $f_{50}$ were 0.3558±0.006 *lp/mm* and 0.2692±0.007 lp/mm for 6 and 18 MV, respectively, values that are significantly better than those recommended by Siemens [35]. The values of $f_{50}$ reported by Luchka (0.391 lp/mm for 6 MV and 0.338 lp/mm for 18 MV) for an aS500 EPID are slightly better in comparison to our results [37]. The difference may relate to the difference in pixel matrix and pixel size. Our EPID consisted of 512×512 pixels with a pixel size of 0.8 $mm^3$ [36], compared to Luchka's 512×384 matrix with a pixel size of 0.78 $mm^3$ [38]. The spatial resolution was reduced for the 18 MV beam due to increased transmission of the high-energy photons through the bar patterns [39] and increased lateral spread of higher energy primary electrons created and the associated broad beam penumbra (figure 4) [32]. The CNR increases with dose rate for 6MV (table 2), due to increase in the difference of pixel values of the brightest and darkest regions. This increased difference arises because of a corresponding increase in counts/pixel/frame with dose rate for both beam energies [33].

## CONCLUSION

This study shows that compared to Las Vegas phantom, implementation of Milad1 EPID phantom and its associated software allows an automated EPID QA process. However, the software is sensitive to artifacts. The advantage of Milad2 EPID phantom over PTW EPID QC phantom is its smaller size which fits smaller EPIDs such as Varian EPID. These phantoms are independent of the EPID system and provide robust tools for continuous monitoring of image quality parameters as well as dosimetric parameters.

## ACKNOWLEDGEMENTS

*The authors would like to acknowledge the radiation oncology department of Isfahan Milad Hospital for supporting this research. The authors wish also thanks Mr. Farsmadan for his technical support.*

## REFERENCES

1. O'Daniel JC, Garden AS, Schwartz DL, Wang H, Ang KK, Ahamad A, Rosenthal DI, Morrison WH, Asper JA, Zhang L, Tung SM, Mohan R, Dong L (2007) Parotid gland dose in intensity modulated radiotherapy for head and neck cancer: Is what you plan what you get? *Int J Radiat Oncol Biol Phys*, ***69**: 1290–6.*
2. Chao KS, Deasy JO, Markman J, Haynie J, Pere CA, Purdy JA, Low DA (2001) A prospective study of salivary function sparing in patients with head-and-neck cancers receiving intensity-modulated or three-dimensional radiation therapy: Initial results. *Int J Radiat Oncol Biol Phys*, ***49**: 907–16.*
3. Bedford JL (2009) Treatment planning for volumetric modulated arc therapy. *Med Phys*, ***36**: 5128–38.*
4. Feygelman VZ and Stevens C (2010) Initial dosimetric evaluation of SmartArc-A novel VMAT treatment planning module implemented in a multi-vendor delivery chain. *J Appl Clin Med Phys*, ***11**: 99-116.*
5. Fredh A, Korreman S, Rosenschold PM (2010) Automated analysis of images acquired with electronic portal imaging device during delivery of quality assurance plans for inversely optimized arc therapy. *Radiother Oncol*, ***94**: 195-8.*
6. *Mohammadi M, Bezak E, Reich P (2006) Comparison of two-dimensional transmitted dose maps: evaluation of existing algorithms. Australas Phys Eng Sci Med, **29:** 179-187.*
7. Kirby M and Glendinning AG (2006) Developments in electronic portal imaging systems. *Br J Radiol*, **79**: 50-65.
8. Mohammadi M, Bezak E, Reich P (2008) Verification of dose delivery for a prostate sIMRT treatment using a SLIC – EPID. *Appl Radiat Isot, **66:** 1930– 8.*
9. Das I, Cao M, Cheng C, Misic V, Scheuring K, Schüle E, Johnstone P (2011) A quality assurance phantom for electronic portal imaging devices. *J Appl Clin Med Phys*, ***12**: 391-403.*

10. van Herk M and Meertent H (1988) A Matrix ionization chamber imaging device for on-line patient setup verification during radiotherapy. *Radiother Oncol*, ***11**: 369-78.*
11. Kirby M and Williams P (1995) The use of an electronic portal imaging device for exit dosimetry and quality control measurements. *Int J Radiat Oncol Biol Phys, **31**: 593-603.*
12. Essers M, Hoogervorst BR, van Herk M, Lanson H, Mijnheer BJ (1995) Dosimetric characteristics of a liquid-filled electronic portal imaging device. *Int J Radiat Oncol Biol Phys*, ***33**: 1265-72.*
13. Heijmen BJ, Pasma KL, Kroonwijk M, Althof VG, de Boer JC, Visser AG, Huizenga H (1995) Portal dose measurement in radiotherapy using an electronic portal imaging device (EPID). *Phys Med Biol*, ***40**:1943-55.*
14. Zhu Y, Jiang XQ, Van Dyk J (1995) Portal dosimetry using a liquid ion chamber matrix: dose response studies. *Med Phys*, ***22**: 1101-6.*
15. Boellaard R, van Herk M, Mijnheer BJ (1996) The dose response relationship of a liquid-filled electronic imaging device. *Med Phys*, ***23**: 1601-11.*
16. Essers M, Boellaard R, van Herk M, Lanson H, Mijnheer BJ (1996) Transmission dosimetry with a liquid- filled electronic portal imaging device. *Int J Radiat Oncol Biol Phys*, ***34**: 931-41.*
17. Leong J (1986) Use of digital fluoroscopy as an on-line verification device in radiationtherapy. *Phys Med Biol*, ***31**: 985-92.*
18. Graham ML, Cheng AY, Geer LY, Binns WR, Vannier MW, Wong JW (1991) A method to analyze 2-dimensional daily radiotherapy portal images from an on-line fiber optic imaging system. *Radiat Oncol Biol Phys*, ***20**: 613-19.*
19. Kirby MC and Williams PC (1993) Measurement possibilities using an electronic portal imaging device. *Radiother Oncol*, ***29**: 237-43.*
20. Kaatee RS, Olofsen MJ, Verstraate MB, Quint S, Heijmen BJ (2002) Detection of organ movement in cervix cancer patients using a fluoroscopic electronic portal imaging device and radiopaque markers. *Int J Radiat Oncol Biol Phys*, ***54**: 576-83.*
21. Mohammadi M and Bezak E (2005) The physical characteristics of a SLIC-EPID for transmitted dosimetry. *Iran J Radiat Res*, **2**: 175-83.
22. Hansen VN, Evans PM, Swindell W (1996) The application of transit dosimetry to precision radiotherapy. *Med Phys*, ***23**: 713-21.*
23. Symonds-Tayler JRN, Partridge M, Evans PM (1997) An electronic portal imaging device for transit dosimetry. *Phys Med Biol*, ***42**: 2273-83.*
24. Parsaei H, el-Khatib E, Rajapakshe R (1998) The use of an electronic portal imaging system to measure portal dose and portal dose profiles. *Med Phys*, ***25**: 1903-9.*
25. Pasma KL, Kroonwijk M, De Boer JC, Visser AG, Heijmen BJ (1998) Accurate portal dose measurement with a fluoroscopic electronic portal imaging device (EPID) for open and wedged beams and dynamic multileaf collimation. *Phys Med Biol*, ***43**: 2047-60.*
26. Bogaerts R, Van Esch A, Reyman R, Huyskens D (2000) A method to estimate the transit dose on the beam axis for verification of dose delivery with portal images. *Radiother Oncol*, ***54**: 39-46.*
27. Rowshanfarzad P, Sabet M, Barnes MP, O'Connor DJ, Greer PB (2012) EPID-based verification of the MLC performance for dynamic IMRT and VMAT. *Med Phys*, ***39**: 6192-207.*
28. Adamson J and Wu Q (2012) Independent verification of gantry angle for pre-treatment VMAT QA using EPID. *Phys Med Biol*, ***57**: 6587-600.*
29. Herman MG, Balter JM, Jaffray DA, McGee KP, Munro P, Shalev S, van Herk M, Wong JW (2001) Clinical use of electronic portal imaging: report of AAPM Radiation Therapy Committee Task Group 58. *Med Phys*, **28**: 712-37.
30. Langmack KA (2001) Portal imaging. *Br J Radiol*, ***74**: 789-804.*
31. Low DA, Klein EE, Maag DK, Umfleet WE, Purdy JA (1996) Commissioning and periodic quality assurance of a clinical electronic portal imaging device. *Int J Radiat Oncol Biol Phys*, ***34**: 117-23.*
32. Rajapakshe R, Luchka K, Shalev S (1996) A quality control test for electronic portal imaging devices. *Med Phys*, ***23**: 1237-44.*
33. Menon G and Sloboda R (2004) Quality assurance measurements of a-Si EPID performance. *Med Dosim*, ***29**: 11-7.*
34. Bulmer N, Budgell G, Clements R, Glendinning A, Kirby M, Sage J, Weston S 2003 Evaluation of iView and iViewGT using the QC-3V phantom. a multicentre study *Proc. of PIPSPro User Meeting (Manchester, UK) pp 7–8.*
35. Mc Garry C, Grattan M, Cosgrove V (2007) Optimization of image quality and dose for Varian aS500 electronic portal imaging devices (EPIDs). *Phys Med Biol*, ***52**: 6865-77.*
36. Nijsten S, van Elmpt W, Jacobs M, Mijnheer B, Dekker A (2007) A global calibration model for a-Si EPIDs used for transit dosimetry. *Med Phys*, ***34**: 3872-84.*
37. Luchka K Letter to the editor. *PIPS News*, 4(3), 2001.
38. Grein EE, Lee R, Luchka K (2002) An investigation of a new amorphous silicon electronic portal imaging device for transit dosimetry. *Med Phys, **29**: 2262-8.*
39. Munro P, Rawlinson JA, Fenster A (1990) Therapy Imaging: A signal-to-noise of a fluroscopic imaging system for radiotherapy localization. *Med Phys*, ***17**: 763-72.*